Intranasal Adeno-Associated Virus Mediated Gene Delivery and Expression of Human Iduronidase in the Central Nervous System: A Noninvasive and Effective Approach for Prevention of Neurologic Disease in Mucopolysaccharidosis Type I

Lalitha R. Belur,[1,*] Alexa Temme,[1] Kelly M. Podetz-Pedersen,[1] Maureen Riedl,[2] Lucy Vulchanova,[2] Nicholas Robinson,[3,†] Leah R. Hanson,[4] Karen F. Kozarsky,[5,‡] Paul J. Orchard,[6] William H. Frey II,[4] Walter C. Low,[7] and R. Scott McIvor[1]

[1]*Center for Genome Engineering, Department of Genetics, Cell Biology and Development;* [2]*Department of Neuroscience;* [3]*Department of Research Animal Resources;* [6]*Program in Blood and Marrow Transplantation, Department of Pediatrics;* [7]*Department of Neurosurgery and Graduate Program in Neuroscience; University of Minnesota, Minneapolis;* [4]*HealthPartners Neurosciences, Regions Hospital, St. Paul, Minneapolis;* [5]*REGENXBIO, Inc., Rockville, Maryland.*
[†]*Present address: Department of Biomedical Sciences, Cummings School of Veterinary Medicine at Tufts University, North Grafton, Massachusetts.*
[‡]*Present address: Vector BioPartners LLC, Bala Cynwyd, Pennsylvania.*

Mucopolysaccharidosis type I (MPS I) is a progressive, multi-systemic, inherited metabolic disease caused by deficiency of α-L-iduronidase (IDUA). Current treatments for this disease are ineffective in treating central nervous system (CNS) disease due to the inability of lysosomal enzymes to traverse the blood–brain barrier. A noninvasive and effective approach was taken in the treatment of CNS disease by intranasal administration of an IDUA-encoding adeno-associated virus serotype 9 (AAV9) vector. Adult IDUA-deficient mice aged 3 months were instilled intranasally with AAV9-IDUA vector. Animals sacrificed 5 months post instillation exhibited IDUA enzyme activity levels that were up to 50-fold that of wild-type mice in the olfactory bulb, with wild-type levels of enzyme restored in all other parts of the brain. Intranasal treatment with AAV9-IDUA also resulted in the reduction of tissue glycosaminoglycan storage materials in the brain. There was strong IDUA immunofluorescence staining of tissue sections observed in the nasal epithelium and olfactory bulb, but there was no evidence of the presence of transduced cells in other portions of the brain. This indicates that reduction of storage materials most likely occurred as a result of enzyme diffusion from the olfactory bulb and the nasal epithelium into deeper areas of the brain. At 8 months of age, neurocognitive testing using the Barnes maze to assess spatial navigation demonstrated that treated IDUA-deficient mice were no different from normal control animals, while untreated IDUA-deficient mice exhibited significant learning and navigation deficits. This novel, noninvasive strategy for intranasal AAV9-IDUA instillation could potentially be used to treat CNS manifestations of human MPS I.

Keywords: intranasal, brain, iduronidase, MPS I, AAV, neurocognitive

INTRODUCTION

MUCOPOLYSACCHARIDOSIS TYPE I (MPS I) is an autosomal recessive storage disease caused by deficiency of α-L-iduronidase (IDUA), resulting in accumulation of heparan and dermatan sulfate glycosaminoglycans (GAGs).[1–4] The most common and severe form of MPS I (Hurler syndrome) is a chronic, multi-systemic progressive disease, resulting in cardiomyopathy, skeletal abnormalities, hepatosplenomegaly, corneal clouding, and pulmonary obstruction. Central nervous system (CNS) complications include hydrocephalus, learning deficits, and mental retardation. If left untreated, the disease results in death by the age of 10 years. Current treatments for MPS I include enzyme replacement therapy (ERT) and allogeneic hematopoietic stem-cell transplantation (HSCT). While early intervention (before 2 years of age) by HSCT

*Correspondence: Dr. Lalitha R. Belur, Center for Genome Engineering, Department of Genetics, Cell Biology, and Development, University of Minnesota, 6-160 Jackson Hall, 321 Church St. S.E., Minneapolis, MN 55455. E-mail: belur001@umn.edu

DOI: 10.1089/hum.2017.187

is associated with prevention of cognitive decline, the procedure is associated with significant morbidity and mortality, and patients continue to exhibit below-normal IQ levels and impaired neurocognitive abilities.[5–15] ERT with the recombinant enzyme laronidase (Aldurazyme) has shown clinical improvement in visceral manifestations of MPS I.[16–20] However, it is ineffective against neurological complications of the disease due to the inability of lysosomal enzymes to traverse the blood–brain barrier (BBB).[20,21] Effective treatment of CNS manifestations of the disease is thus limited by the inability of current therapies to deliver sufficient enzyme to the CNS.

A new and promising approach for delivery of IDUA to the brain in MPS I is by gene transfer,[22,23] either by direct *in vivo IDUA* gene transfer into the CNS or by *ex vivo IDUA* gene transfer into stem cells that subsequently engraft and penetrate the BBB. Neonatal intravenous administration of adeno-associated virus serotype 2 (AAV2) vector,[24] intraparenchymal injections of AAV5,[25] direct intracerebroventricular (ICV) injection of AAV8 vector into newborns,[26] *ex vivo* transduction of hematopoietic stem cells with expression in red blood cells,[27,28] retroviral vector mediated gene therapy into mouse models of MPS I,[29–31] direct neonatal *in vivo* injection of lentiviral vectors,[32] and successful *ex vivo* transduction using lentiviral vectors[33] have resulted in improvements in phenotypic manifestations and/or behavioral dysfunctions of MPS I mice. A comparison of intracarotid (endovascular) and ICV routes of AAV5 administration into MPS I mice resulted in significant increases of IDUA enzyme levels in the brain, although direct ICV injection was significantly better in terms of vector distribution throughout the brain.[34] Direct parenchymal[35] injections into feline and canine[36,37] models of MPS I have also resulted in correction of storage pathology in the CNS. Intravenous injections into MPS I cats using AAV9 or AAVrh.10 also results in expression of enzyme in the brain.[35] While direct injection of vector into the brain yields the most widespread distribution and expression, the invasive nature of this route of delivery is an impediment to its clinical application.

As an alternate, noninvasive route of AAV delivery, intranasal administration has been explored—an approach shown to traffic therapeutic molecules rapidly to the brain via olfactory and trigeminal pathways innervating the nasal passages. The goal of the studies described herein was to test the effectiveness of intranasal AAV9 vector instillation for gene delivery and expression of IDUA in the CNS of MPS I mice. High levels of IDUA enzyme expression are reported in the olfactory bulb and wild-type levels in other parts of the brain after intranasal AAV9-IDUA administration, and the prevention of neurobehavioral spatial navigation dysfunction in adult intranasally treated MPS I mice is also demonstrated. This is the first study to demonstrate intranasal delivery of an AAV9 vector to the brain effectively. The results demonstrate the feasibility of achieving correction of metabolic disease and neurologic dysfunction after noninvasive intranasal delivery of AAV vector applicable to lysosomal diseases and other disorders in neurologic function.

MATERIALS AND METHODS

AAV9-MCI vector

Generation of the miniCAGS regulated IDUA (MCI) expression cassette has been described previously.[26] This plasmid was packaged into AAV9 virions at the University of Pennsylvania vector core in order to generate recombinant (r) AAV9-IDUA. The vector titer was 1.1×10^{13} genome copies/mL. AAV9-GFP vector was purchased from the University of Pennsylvania vector core, and the titer was 1×10^{13} genome copies/mL.

Animals and intranasal infusions

The MPS I mouse strain was generously provided by Dr. E. Neufeld, and *IDUA*$^{-/-}$ offspring were generated from homozygous *IDUA*$^{-/-}$ breeding pairs. Animals were maintained under specific pathogen-free conditions in AAALAC-accredited facilities. Animal work was reviewed and approved by the Institutional Animal Care and Use Committee of the University of Minnesota. In order to avoid immune response, MPS I IDUA-deficient animals were immunotolerized starting at birth with an intravenous injection of 5.8 μg/g Aldurazyme (Dr. P. Orchard), followed by five subsequent weekly intraperitoneal injections. These immunotolerized MPS I animals were treated intranasally with AAV9-MCI vector at 3 months of age, as previously described.[38] The vector was administered by applying a series of eight 3 μL drops with a micropipette to the nasal cavity of each mouse, alternating between right and left nostril, at 1 min intervals between each nostril, for a total of 24 μL and a full dose of 2.4×10^{11} vector genomes.

IDUA enzyme assay

Animals were sacrificed at 8 months of age ($n=7$ for all groups) and transcardiacally perfused with 50 mL of phosphate-buffered saline (PBS), and the brains were dissected into right and left hemispheres. Each hemisphere was micro-dissected into hippocampus, cerebellum, cortex, striatum, olfactory bulb,

and brain stem. The spinal cord, lung, and liver were also collected. Tissues were frozen on dry ice and stored at –20°C until processed. Tissues were homogenized in 0.9% saline in a Bullet Blender (Storm 24 Homogenizer [MIDSCI]), and homogenates were clarified by centrifugation. Tissue lysates were assayed for IDUA activity in a fluorometric assay using 4-MU iduronide as substrate (Glycosynth, England), as previously described.[26] Emitted fluorescence was measured in a BioTek Synergy Mx plate reader. Protein was measured using the Pierce assay. Enzyme activity is expressed as nmol 4-methylumbelliferone released per mg protein per hour (nmol/mg/h).

Histopathology

For detection of storage vacuoles and toluidine blue staining, 8-month-old treated animals ($n=2$) were sacrificed as described for the IDUA enzyme assay, along with age-matched MPS I ($n=2$) and heterozygous controls ($n=2$). Tissues were fixed and stained with toluidine blue as described previously.[24] Stained sections were scored under blinded conditions for the presence of pathologic storage vesicles. Eight sections per animal were evaluated from each of the different regions of the brain: hippocampus, cerebellum, cortex, striatum, olfactory bulb, midbrain (thalamus, brain stem), as well as the liver and lung. All sections were evaluated in a blinded fashion by a pathologist using a semi-quantitative grading scale assessing the amount of affected cells (1–4+) within each region: 0, no cytoplasmic vacuoles; +, cytoplasmic vacuoles in <10% of cells; ++, cytoplasmic vacuoles in 10–25% of cells; +++, cytoplasmic vacuoles in 25–50% of cells; ++++, cytoplasmic vacuoles in >50% of cells. The types of vacuoles present in affected cells (small, medium, or large) were also assessed.

Immunohistochemistry

At 8 months of age, mice were deeply anesthetized and perfused via the heart with calcium-free Tyrode's solution (in mM: NaCl 116, KCl 5.4, $MgCl_2 \cdot 6H_2O$ 1.6, $MgSO_4 \cdot 7H_2O$ 0.4, NaH_2PO_4 1.4, glucose 5.6, and $NaHCO_3$ 26) followed by fixative (4% paraformaldehyde and 0.2% picric acid in 0.1 M of phosphate buffer, pH 6.9). Tissues were dissected and stored in PBS containing 10% sucrose and 0.05% sodium azide at 4°C for a minimum of 24 h before being frozen and sectioned at 14 μm thickness using a cryostat. Sections were mounted onto gel-coated slides and stored at –20°C until further use. For immunohistochemical staining, sections were incubated in diluent (PBS containing 0.3% Triton X-100; 1% bovine serum albumin, 1% normal donkey serum) for 1 h at room temperature followed by incubation in primary antisera overnight at 4°C. Primary antisera included sheep anti-IDUA (specific for human IDUA; R&D Systems, Minneapolis, MN; 1:500), chicken anti-GFP (Abcam, Cambridge, United Kingdom; 1:1,000), and rabbit anti-olfactory marker protein (OMP; Abcam; 1:100). For GFP immunostaining, $n=3$ (treated), $n=1$ (MPS I, Het). For IDUA immunostaining, $n=4$ (treated), $n=1$ (MPS I, Het). Sections were rinsed in PBS, incubated in species-appropriate secondary antisera (Cy2 1:100, Cy3 1:300, Cy5 1:300; Jackson ImmunoResearch, West Grove, CA) for 1 h at room temperature, rinsed again using PBS, and coverslipped using glycerol and PBS containing p-phenylenediamine (Sigma–Aldrich, St. Louis, MO). Images were collected using an Olympus Fluoview 1000 confocal microscope and adjusted for brightness and color using Adobe Photoshop software.

Barnes maze

At 8 months of age, mice ($n=7$–8 animals per group) were analyzed for neurocognitive deficits and spatial navigation using the Barnes maze. The Barnes maze consisted of a white circular acrylic platform, 92 cm in diameter and elevated 105 cm above the floor, with 40 equally spaced holes (5 cm in diameter) around the perimeter. Each of the holes was closed with a sliding white piece of cardboard underneath the hole, except for one open hole from which a black acrylic escape box underneath could be accessed by means of a sliding white ramp. From the center of the maze all holes appeared identical so that the test animal could not differentiate between the escape hole and the other holes from the center point or from any other point on the maze. However, when test animals were adjacent to the escape hole, they could discriminate between the escape and other holes by looking down into the escape box. Multicolored visual cues were placed around the room in the four cardinal directions: north, south, east, and west. The platform was brightly lit with overhead lighting. The animal was released in the center of the maze with the lights dimmed. The bright overhead lights were turned on, and the mouse was given 3 min to explore the maze. If it did not enter the escape box, it was guided to the escape hole and left there for 30 s before being returned to its home cage. Animals were administered six trials a day for 4 days. Trials were recorded and analyzed using Ethovison software, which allows automated tracking of animals.

RESULTS

Intranasal instillation of AAV9-GFP leads to transduction of nasal epithelium and olfactory bulb

Intranasal delivery of therapeutic molecules for distribution to the brain has three significant benefits compared to other routes of administration: it is non-invasive, it bypasses the BBB, which is a significant impediment to the delivery of therapeutics to the brain, and it reduces systemic exposure and unwanted systemic side effects. A preliminary study was conducted to determine the sites of vector transduction in the brain after intranasal AAV instillation. Two to three months post treatment, animals were sacrificed, and tissues were processed for histologic analysis of GFP expression. While robust GFP immunoreactivity (-ir; Fig. 1) was detected in the olfactory epithelium (Fig. 1A–C) and in the olfactory bulb (Fig. IE and F), GFP-ir cells were not observed anywhere else in the brain. In the olfactory bulb, the strongest expression was observed in the glomerular layer (Fig. 1E and F), the first layer of synaptic processing in the brain for structures emanating from the nasal passage. Co-staining for OMP in the olfactory bulb demonstrated that AAV9 transduction and GFP expression were occurring in mature olfactory sensory neurons of the olfactory bulb (Fig. 2).

Biochemical and metabolic effects of intranasal AAV9-IDUA administration

The effectiveness of intranasal AAV9-IDUA vector instillation for treatment of CNS disease was evaluated in adult IDUA-deficient mice, previously demonstrated to model MPS I in humans. Adult IDUA-deficient mice were intranasally instilled with AAV9-IDUA vector. At 8 months of age, animals were sacrificed, and the brain was micro-dissected into the left and right cortex, striatum, hippocampus, cerebellum, olfactory

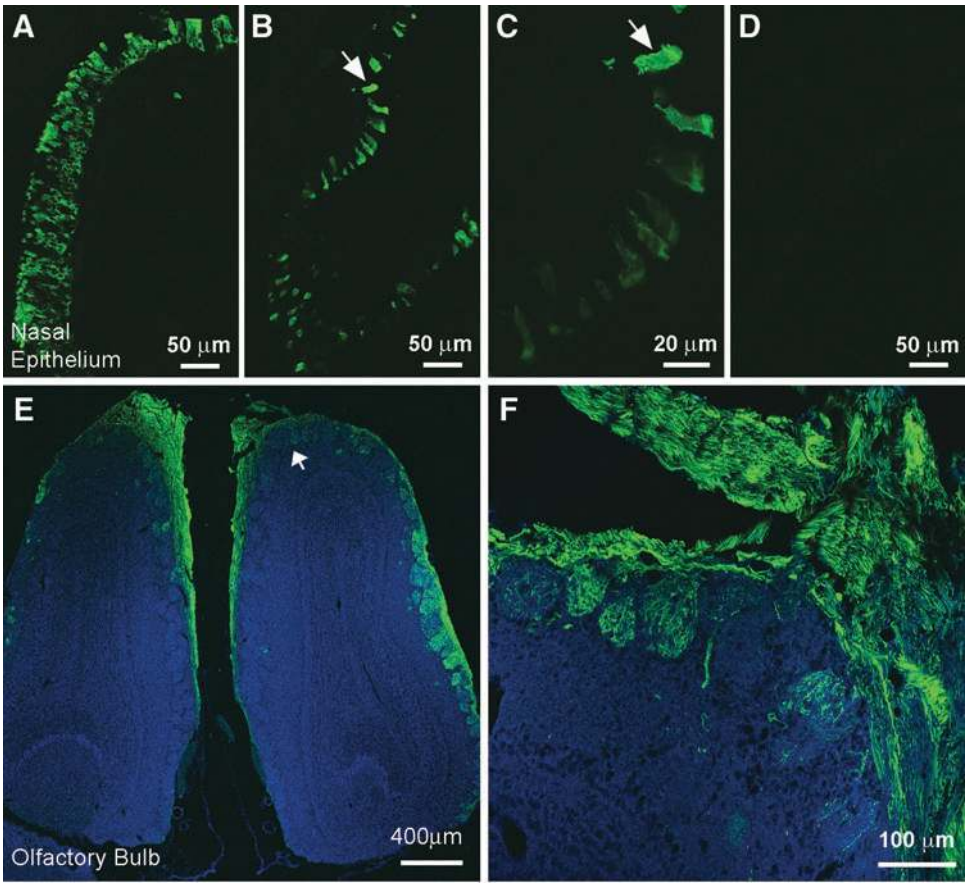

Figure 1. GFP immunofluorescence observed in the olfactory bulb after intranasal administration of AAV9-GFP. Three-month-old mucopolysaccharidosis type I (MPS I) mice ($n=3$) were infused intranasally with an AAV9-GFP vector. At 8 months of age, animals were sacrificed, and the tissues were harvested and evaluated for GFP expression. Extensive GFP-ir (immunoreactivity) is observed in many cells in both rostral and caudal regions of the nasal epithelium **(A–C)**. In some cases, GFP-ir extends into the cilia of nasal epithelial cells (**B**, higher magnification in **C**). No labeling was seen in the nasal epithelium from control animals that did not receive virus **(D)**. Extensive GFP-ir is also seen in the glomeruli of the olfactory bulb after intranasal delivery of AAV9-GFP (*green*; **E** and **F**). Structures in *blue* are background fluorescence imaged using filter set for UV. Scale bars A, B, and D = 50 μm, C = 20 μm, E = 400 μm, F = 100 μm.

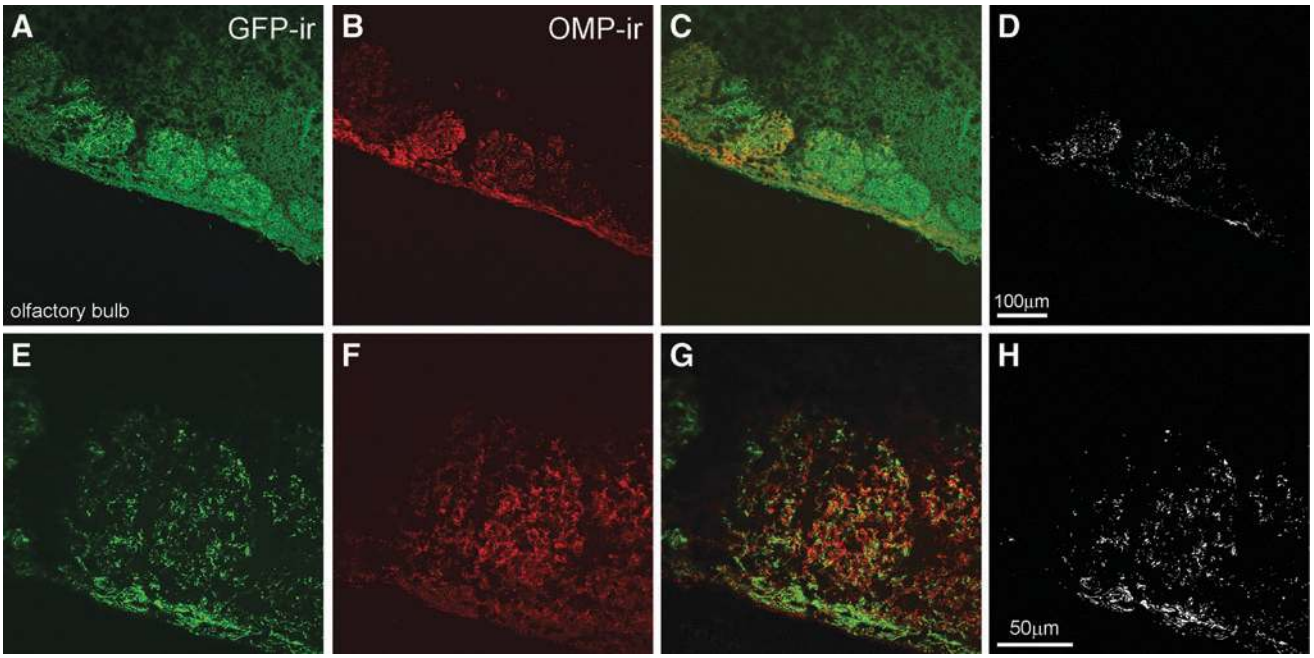

Figure 2. Expression of GFP in neurons after intranasal infusion of AAV9-GFP. Tissue sections from MPS I mice intranasally administered AAV9-GFP vector were co-stained for GFP and for olfactory marker protein (OMP), which is expressed exclusively in the olfactory bulb in the brain (described in Materials and Methods). Higher magnification images demonstrate that GFP-ir (*green*; **A** and **E**) and OMP-ir (*red*; **B** and **F**) are distinctly co-localized in glomeruli of the olfactory bulb (*yellow*; **C** and **G**), demonstrating AAV9-GFP transduction in OMP-positive neurons. Due to the high intensity of GFP staining, the *green* and *red* images were thresholded separately, and images were merged (using the Photoshop function "multiply"). The overlapping pixels where co-localization is present are shown in *white* (**D** and **H**). Scale bars A–D = 100 μm, E–H = 50 μm.

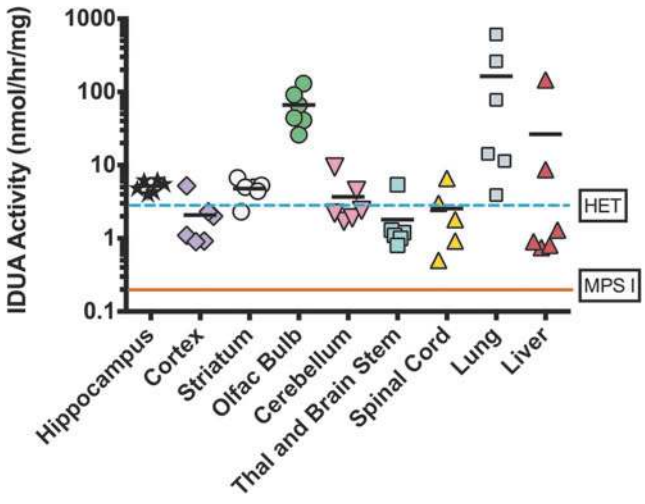

Figure 3. Intranasal infusion of AAV9-α-L-iduronidase (IDUA) restores IDUA enzyme activity in the brain and lung. Five months after intranasal infusion of AAV9-IDUA into MPS I mice, animals were euthanized. The brains were micro-dissected into the cortex, olfactory bulb, striatum, hippocampus, cerebellum, spinal cord, and thalamus + brainstem, and extracts were assayed for IDUA enzyme activity. The levels of IDUA enzyme were determined in AAV9-IDUA-treated MPS I mice (n=6), IDUA heterozygote mice (n=3), and in untreated MPS I animals (n=3) as indicated. The dashed line indicates enzyme levels in heterozygote controls, while the solid line represents IDUA activity in MPS I control animals.

bulb and brain stem/thalamus. Tissue extracts were prepared and assayed for IDUA enzyme expression using fluorogenic 4MU iduronide substrate, as previously described[26] (Fig. 3). Untreated IDUA-deficient mice had no detectable enzyme in tissue extracts from any part of the brain. In contrast, IDUA-deficient mice treated intranasally with AAV9-IDUA vector exhibited IDUA enzyme activity levels in the olfactory bulb that ranged from 10- to 50-fold that of wild-type mice. Other parts of the brain, which included the hippocampal formation, showed wild-type or close to wild-type levels of IDUA. Enzyme levels ranged from wild type to 100$\times$wild type in the lung, and from 15% wild type to 30$\times$wild type in the liver. IDUA activity was not detected in the plasma of treated animals, except for one mouse that had a low level of 67 nmol/h/mL of activity.

Tissue samples were sectioned and stained with toluidine blue to evaluate the effect of intranasal AAV9-IDUA vector treatment on accumulation of lysosomal storage material (Fig. 4). General observations of the vesicle type in affected cells in different tissues is shown in Table 1. The midbrain and cortex of the brain had vacuoles that were present within the neurons and glial cells as well as

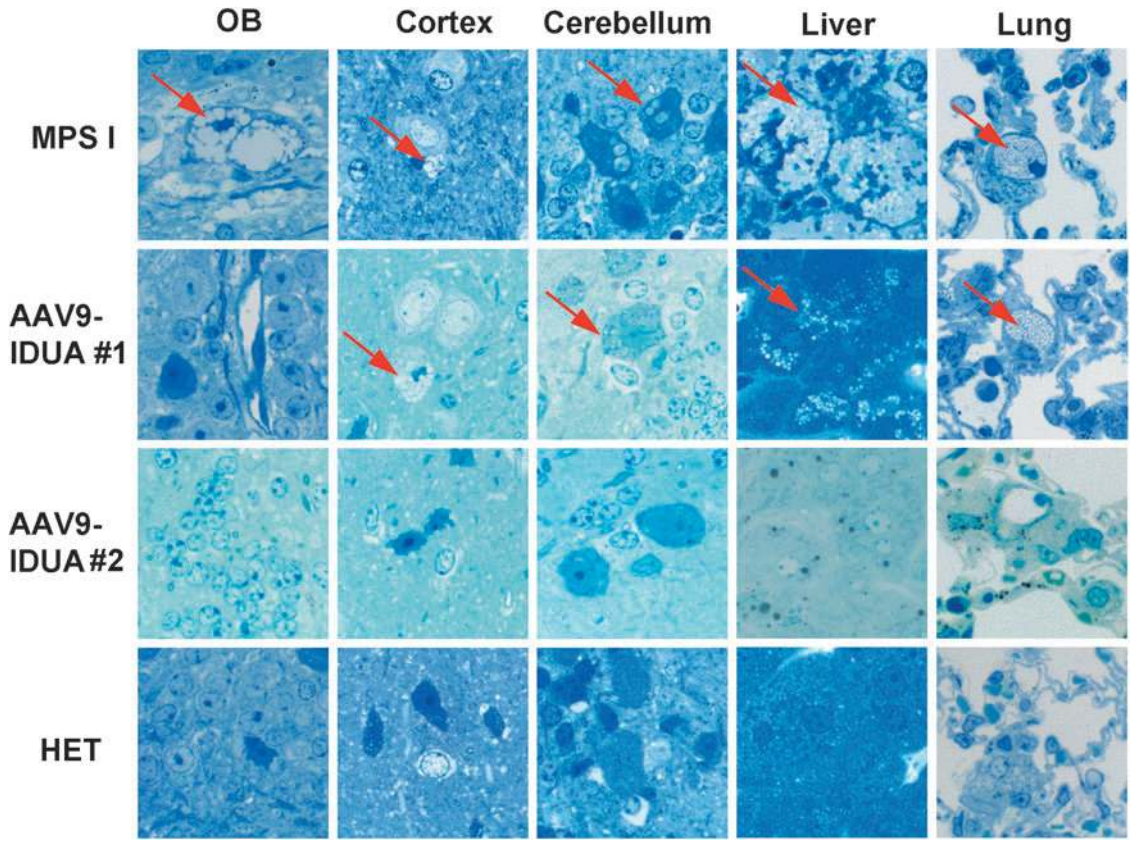

Figure 4. Reduction in lysosomal storage material following intranasal administration of AAV9-IDUA. Animals were sacrificed 5 months after intranasal instillation, and histopathological analysis of tissue sections for storage material was carried out using toluidine blue staining, as described in the Materials and Methods. *Arrows* indicate cytoplasmic vacuolization. Extensive vacuolization was seen in all tissues in MPS I animals, while AAV9-IDUA-treated animals show mixed results. Animal 1 exhibited no storage-related pathology in the olfactory bulb and had reduced storage material in all other parts of the brain compared to untreated controls. Animal 2 had no observable storage-related pathology in any part of the brain ($n=2$, all groups).

perivascular cells. Within the cerebellum, the vacuoles were only present within Purkinje cells, with vacuole sizes generally medium- or large-sized compared to all other cells where they were predominantly small or occasionally medium. Within the liver, vacuoles were present in both hepatocytes and also in Kupffer cells, and in the lung, vacuoles were present within the pulmonary macrophages. All vacuoles in the liver and lung were of the small type. Control, untreated MPS I mice exhibited significant lysosomal distension in the olfactory bulb, cortex, cerebellum, liver, and lung. In contrast, all MPS I mice treated intranasally with AAV9-IDUA vector exhibited reduced storage material in the olfactory bulb but showed mixed results with respect to vacuolar pathology in the cortex and cerebellum. Treated animal #1, which demonstrated lower than normal IDUA enzyme activity in the brain (with the exception of olfactory bulb), showed clearance of storage material in the olfactory bulb, but lysosomal pathology was present in the cerebellum and cortex, similar to IDUA-deficient animals. However, as shown in Table 1, the size of storage vacuoles was reduced

Table 1. *Description of vesicle type within affected cells*

Animal	*Hipp*	*Cbllm*	*Ctx*	*Striatum*	*Olf Bulb*	*Med/Th/BS*	*Lung*	*Liver*
Treated #1	Sml	Sml	Sml	Sml–med	Sml	Sml	Sml	Sml–med
Treated #2	Sml–med	NA	Sml	Sml	Sml	Sml	Sml	NA
Het	Sml	Sml–med	NA	Sml	Sml	NA	NA	NA
MPS I	Sml–med	Lrg	Sml-med	Med–lrg	Sml–med	Sml–med	Sml	Sml–med

Sml, small; med, medium; lrg, large; NA, not applicable; Ctx, cortex; Cbllm, cerebellum; Hipp, hippocampus; Olf bulb, olfactory bulb; Med, medulla; Th, thalamus; BS, brain stem.

in treated animal #1. Another treated animal (#2) showed very little to no pathology in the brain, similar to that of the Het controls. A semi-quantitative grading scale to describe cell density is presented in Table 2. Treated animal #1 had the highest score (of cells affected) in every location analyzed, similar to that of the IDUA-deficient controls. Affected cells within the liver were >50% in both treated animal #1 and the untreated MPS I control mice. This was in stark contrast to treated animal #2 and Het controls, both of which had no affected cells and had similar scores in all locations, with 1+ or 0 except for cerebellum (Het 2+) and striatum (treated animal #2 2+). Pulmonary macrophages were observed in treated animal #1 (4+), whereas the Het control, treated animal #2, and MPS I animals had 0, 1+, and 2+ macrophage scores, respectively. These results demonstrate the potential of intranasal AAV vector for correction of abnormal storage pathology in the CNS, liver, and lungs.

Immunohistological analysis shows IDUA staining of nasal epithelium and olfactory bulb

Immunofluorescence staining for IDUA (Fig. 5) demonstrated a pattern similar to the staining seen after infusion of the AAV9-GFP vector. Strong IDUA staining was observed in the nasal epithelium (Fig. 5A–D) and olfactory bulb (Fig. 5G–J), but there was no evidence for the presence of transduced cells in other brain regions. A low level of IDUA transduction was also observed in the lung (Fig. 5M–P) and liver (Fig. 5S–V). No positive IDUA staining was observed in other peripheral organs. These results indicate that IDUA enzyme activity in the CNS most likely occurred as the result of AAV9-IDUA transduction and *IDUA* gene expression in the nasal epithelium and in the olfactory bulb, with subsequent enzyme diffusion from these sites of expression into caudal regions of the brain.

Prevention of neurocognitive spatial navigation dysfunction in animals treated intranasally with AAV9-IDUA

At 8 months of age, intranasally treated MPS I animals along with age-matched heterozygote and IDUA-deficient control animals were tested for neurocognitive function using the Barnes maze[39,40] in order to assess spatial navigation performance (Fig. 6). In this test, animals are placed in the middle of a circular platform with 40 holes around the perimeter of the platform, but only one of the holes is open, therefore allowing the animal to escape. Test animals are expected to exhibit a reduction in time required to find the escape hole through repeated trials (six trials a day for 4 days) by using extra-maze visual cues. Unaffected heterozygote animals exhibited improved performance over the 4-day period of testing, while MPS I mice displayed a deficit in learning this task and locating the escape hole. Remarkably, MPS I mice treated intranasally with AAV9-IDUA exhibited behavior similar to the heterozygote controls. There was no significant difference between the normal heterozygote animals and the intranasally treated MPS I animals, while latency to escape was significantly reduced between these two groups and untreated MPS I animals. It is concluded from these results that intranasal administration of AAV9-IDUA prevented emergence of the neurocognitive deficit seen in untreated MPS I animals.

DISCUSSION

Normal or close to normal levels of IDUA enzyme were observed in all parts of the brain following intranasal instillation of AAV9-IDUA vector to MPSI mice. Levels of IDUA were highest in the olfactory bulb, which was consistent with immunofluorescence staining using both IDUA and GFP antibodies. Immunofluorescence results also demonstrated that transduction was limited to the olfactory bulb and that enzyme activity in other parts of the brain is most likely the result of enzyme diffusion from the olfactory lobe.

Lysosomal storage diseases, in particular the MPSs, are ideal candidates for gene therapy. Each MPS is a monogenic recessive disorder, and it has been demonstrated that even a small amount of enzyme expression (<10%) is sufficient to have a clinical impact on the disease. One of the most promising features of MPSs for gene therapy is the unique physiological condition termed "cross-correction."[41,42] In this condition, the lysosomal enzyme is expressed and secreted into the extracellular space, where it is subsequently taken up via mannose 6-phosphate receptors expressed on the surface of neighboring cells and trafficked to lysosomes where it contributes to lysosomal metabolism, thereby bringing about "cross-correction." Therefore, by eliciting supraphysiological levels of enzyme expression in a small number of cells, it is possible for secreted enzyme to diffuse through tissues and be taken up by a variety of cell types in distant locations, thus providing clinical benefit.

The availability of small and large animal models mimicking the main features of human MPS disease has contributed significantly in evaluating therapeutic strategies. There are several preclinical strategies of AAV infusion for CNS disease that

Table 2. *Summary of tissue pathology*

Animal	*Hipp*	*Cbllm*	*Ctx*	*Striatum*	*Olf Bulb*	*Med/Th/BS*	*Lung*	*Liver*
Treated #1	++++	++++	+	+++	++	+	++++	++++
Treated #2	+	0	+	++	+	+	+	0
Het	+	++	0	+	+	0	0	0
MPS I	++++	++++	+	+++	+++	+	++++	++++

Stained sections were evaluated for presence of pathologic storage vesicles under blinded conditions. The grading scheme describes the distribution of affected cells as a proportion of total cells. For the lung, the evaluation was as a proportion of total macrophages present, while for the cerebellum it was assessed in Purkinje cells only.

0, no cytoplasmic vacuoles; +, cytoplasmic vacuoles in <10% of cells; ++, cytoplasmic vacuoles in 10–25% of cells; +++, cytoplasmic vacuoles in 25–50% of cells; ++++, cytoplasmic vacuoles in >50% of cells.

have been developed and tested in animal models of MPS disease. Intraparenchymal (striatal) delivery of AAV2 and AAV5 has been used to treat MPS I in mice and dogs,[25] showing that direct delivery into the tissue can lead to widespread dissemination of vector, resulting in biochemical and histological correction in the brain, neurologic improvement, and extended life-span. ICV[26] and IT[43] infusions of AAV8 and AAV2, respectively, into the CSF of MPS I mice and of AAV9 into MPS I cats[35] and dogs[36] have shown therapeutic benefits with favorable phenotypic outcomes. The reported ability of AAV9 and AAVrh.10 serotypes to cross the BBB has led to the exploration of intravenous injections for treatment of MPS disease. Intravenous administration of AAV8 for MPS I cats[44] has been tested and

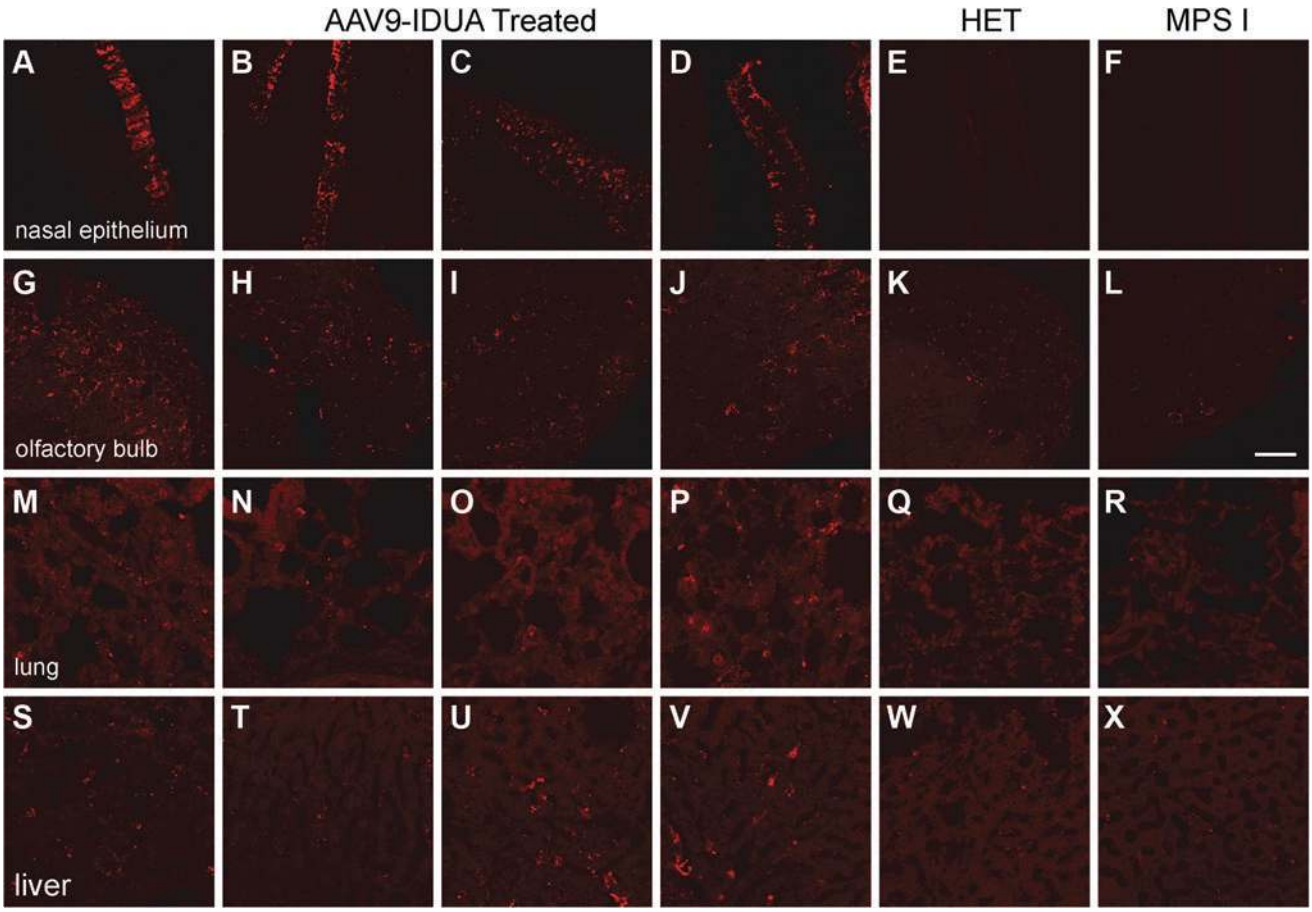

Figure 5. Brain IDUA immunofluorescence observed only in the olfactory bulb after intranasal infusion of AAV9-IDUA. Tissue sections were prepared from MPS I mice intranasally administered AAV9-IDUA and stained with an anti-human IDUA antibody ($n=4$). Immunofluorescence images reveal intensely stained nasal epithelium **(A–F)**, while brain sections reveal robust staining in the olfactory bulb **(G–L)**. A low level of IDUA immunostaining is also seen in the lung **(M–R)** and liver **(S–X)**. Specificity of the IDUA antisera is confirmed by the lack of staining in the MPS I ($n=1$) **(F, L, R, X)** and Het animals ($n=1$) **E, K, Q, W**. Scale bar = 50 μm. There was no IDUA staining observed elsewhere in the brain or other peripheral organs (images not shown).

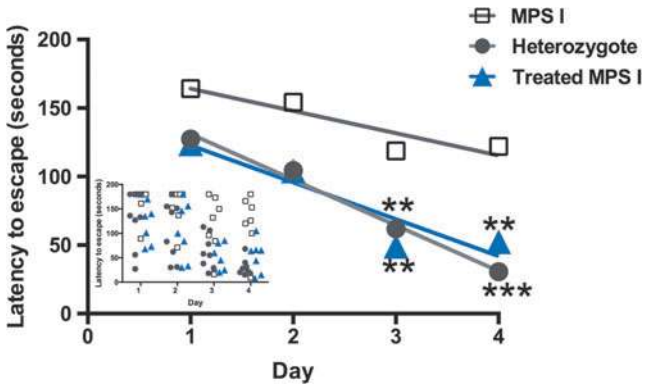

Figure 6. Improved neurocognitive function in intranasally treated animals. The Barnes maze was used to assess spatial learning and memory. As described in Materials and Methods, animals had to locate the escape hole on the maze, and were subjected to six trials a day for 4 days. The inset depicts escape times in individual animals, while sample means are represented in the main graph. MPS I mice ($n=8$) displayed a significant neurocognitive deficit in locating the escape hole compared to heterozygote controls ($n=8$; ***$p<0.0001$), while intranasally treated animals ($n=7$) behaved similarly to heterozygote controls and significantly better than untreated MPS I mice (**$p<0.002$).

shown to have a beneficial effect on CNS pathology. However, the efficiency of CNS transduction after intravenous AAV vector administration is not as robust as direct injection into the CNS, and a large dose of vector is required to have a therapeutic effect in the CNS.

While intraparenchymal, intracerebroventricular, and intrathecal (cisterna magna) gene delivery approaches for MPS I have demonstrated neurologic efficiency, they are highly invasive and are not ideal routes of administration. Intranasal gene delivery to the brain provides a noninvasive route of administration along the olfactory and trigeminal nerve pathways, and has the distinct added advantage of bypassing the BBB while reducing systemic exposure.[45] The pathways and mechanisms of substance delivery from the nose to brain are not fully understood. Molecules enter the olfactory bulb/brainstem by an intracellular or para-cellular route along the olfactory and/or trigeminal nerves, both of which enervate the nasal passages.[46–53] AAV 2 vector has been administered intranasally to mice for treatment of depression with promising results.[54] Previous work has shown that after intranasal delivery of the 85kD IDUA enzyme Aldurazyme, IDUA enzyme was detected in all areas of the brain, with levels ranging from 5% to 26% of wild-type mice.[38] In the same study, IDUA enzyme expression was also detected in the brain after intranasal delivery of AAV8-IDUA vector, especially in the olfactory bulb, which had five times the amount of enzyme compared to wild type. IDUA enzyme levels in other parts of the brain were low (approximately 2% of wild type) and were undetected histologically, probably due to the lack of vector transduction in the brain or transduction at levels that were too low to detect. This is the first study showing effective transduction of the brain after intranasal delivery of an AAV9 vector associated with improved neurocognitive function. In this study, IDUA levels were significantly higher than those previously observed,[38] with enzyme levels in the olfactory lobe at an average of 40-fold higher than wild-type animals, and normal to double the levels of enzyme in the hippocampus, striatum, and cerebellum. Enzyme levels in the cortex, thalamus, and brain stem were 50% that of wild-type animals, while in the spinal cord, enzyme levels ranged from 20% to twice the normal level of enzyme. Enzyme expression was also observed in the lung, which could be due to leakage of vector into the lung during the nasal instillation process. It has also been proposed that intranasally delivered substances that are absorbed by the intranasal lamina propria but do not enter into nasal capillaries may drain into deep cervical lymph nodes in the neck, from whence they flow to the heart and eventually to the lung and liver. This could be an explanation for the levels of enzyme seen in the liver, and could also contribute to enzyme levels in the lung. While IDUA transduction was also detected in both the lung and liver, these levels were low, especially compared to transduction levels in the liver following intravenous administrations of AAV9-IDUA (90–95% transduction efficiency,[55] and enzyme levels approximately 1,000-fold above background; data not shown). The low level of transduction observed in liver and lung after intranasal instillation is possibly insufficient to result in detectable IDUA secretion into the circulation, which is why no enzyme was seen in the plasma (except for one animal). GFP and IDUA expression were detected histologically in the nasal epithelium and in the olfactory bulb but not anywhere else in the brain. However, correction of enzyme deficit in other parts of the brain suggests that the olfactory bulb and/or the nasal epithelium possibly serve as a storage depot for vector transduction and enzyme expression, followed by IDUA diffusion and subsequent uptake of enzyme in other parts of the brain by metabolic cross-correction. Lack of histological staining for diffused IDUA enzyme that has been taken up by cells in other parts of the brain is due to low levels of enzyme that are beyond the limit of histological detection. The primary difference between the previous[38] and current study is the serotype of AAV used: AAV8 versus AAV9. While both serotypes transduce

the CNS quite efficiently, a comparative assessment of transduction profiles at different ages and using different routes of administration shows that AAV9 transduces most cell types and areas in the CNS better than AAV8, with the exception of glial cells.[56]

The prevention of cognitive deficits in spatial navigation that was observed in MPS I mice with intranasal AAV9-IDUA administration is best explained by restoration of IDUA levels in the hippocampal formation. The role of the hippocampus as a cognitive map of the external environment is well established in mammals.[57,58] This area of the brain enables mice and rats to navigate mazes by utilizing visual cues that aid in the formation of so-called "place fields" by neurons in the hippocampus,[58] and the aggregate of hippocampal neurons and their associated place fields represent a cognitive map of the Barnes maze. It is possible that in the absence of IDUA, the resulting biochemical abnormalities cause hippocampal neurons to be less proficient in the formation of highly resolved place fields that would be required for determining the location of a small escape hole in the Barnes maze. The restoration of IDUA levels in the hippocampus by intranasal instillation of AAV9-IDUA may therefore be sufficient to re-establish normal physiological function and place-field formation by neurons in the hippocampus, thus allowing treated animals to navigate to the escape hole in the maze efficiently.

Despite the overall success of intranasal AAV9-IDUA delivery in treating MPS I, there are several limitations and questions that must be addressed before this method can be translated to the treatment of human disease. Improvement in the efficiency of vector delivery to the CNS is a primary factor. It is unknown if there is a limitation on the size of molecules that can be delivered from the nose to the CNS. Studies with dextrans of various sizes indicate that there is an inverse relationship between size and efficiency of delivery following intranasal administration.[46,47] Mechanistic questions regarding the route of AAV distribution after intranasal administration—intracellular, para-cellular, or a combination of the two—need to be addressed. The key to success using this route of delivery will be understanding the underlying mechanism of transport from nose to brain, which may lead to improved efficiency of delivery. The results from this study demonstrate that intranasal administration is highly promising as an alternative to current modalities of AAV vector treatment due to its noninvasive nature and ease of delivery in patients, and is widely applicable not just to the mucopolysaccharidoses but also to a wide variety of neurological disorders as well.

ACKNOWLEDGMENTS

For histopathological staining, we thank the Characterization Facility at the University of Minnesota, a member of the NSF-funded Materials Research Facilities Network (www.mrfn.org) via the MRSEC program. Behavioral studies were performed in the Mouse Behavior Core at the University of Minnesota (supported by NIH grant NS062158). We thank core director Dr. Benneyworth for help with the Barnes maze testing. We thank Drs. Aronovich, Hackett, and Whitley for helpful advice on the manuscript, and B. Koniar for excellent animal care. This study has been previously presented at conferences, and has been published in abstract form in conference proceedings. This study was funded by grants HD032652 and DK094538 from the National Institutes of Health.

AUTHOR DISCLOSURE

K.K. currently consults for and receives compensation from REGENXBIO, Inc. No competing financial interests exist for the remaining authors.

REFERENCES

1. Scott HS, Bunge S, Gal A, et al. Molecular genetics of mucopolysaccharidosis type I: diagnostic, clinical, and biological implications. Hum Mutat 1995;6:288–302.
2. Wraith JE, Jones S. Mucopolysaccharidosis type I. Pediatr Endocrinol Rev 2014;12:102–106.
3. Neufeld EF, Muenzer J. The mucopolysaccharidoses. In: Beaudet AL, Scriver CR, Sly WS, Valle D, eds. The Metabolic and Molecular Bases of Inherited Disease. New York: McGraw Hill: 2001:3421–3452.
4. Muenzer J. Overview of the mucopolysaccharidoses. Rheumatol 2011;50:4–12.
5. Krivit W, Sung JH, Shapiro EG, et al. Microglia: the effector cell for reconstitution of the central nervous system following bone marrow transplantation for lysosomal and peroxisomal storage diseases. Cell Transplant 1995;4:385–392.
6. Krivit W. Allogeneic stem cell transplantation for the treatment of lysosomal and peroxisomal metabolic diseases. Springer Sem Immunopathol 2004;26:119–132.
7. Orchard PJ, Blazar BR, Wagner J, et al. Hematopoietic cell therapy for metabolic disease. J Pediatrics 2007;151:340–346.
8. Peters C, Steward CG; National Marrow Donor Program; International Bone Marrow Transplant

Registry, Working Party on Inborn Errors, European Bone Marrow Transplant Group. Hematopoietic cell transplantation for inherited metabolic diseases: an overview of outcomes and practice guidelines. Bone Marrow Transplant 2003;31: 229–239.

9. Unger ER, Sung JH, Manivel JC, et al. Male donor-derived cells in the brains of female sex-mismatched bone marrow transplant recipients: a Y-chromosome specific in situ hybridization study. J Neuropathol Exp Neurol 1993;52:460–470.
10. Hess DC, Abe T, Hill WD, et al. Hematopoietic origin of microglial and perivascular cells in brain. Exp Neurol 2004;186:134–144.
11. Prasad VK, Kurtzberg J. Transplant outcomes in mucopolysaccharidoses. Semin Hematol 2010;47: 59–69.
12. Peters C, Balthazor M, Shapiro EG, et al. Outcome of unrelated donor bone marrow transplantation in 40 children with Hurler syndrome. Blood 1996; 87:4894–4902.
13. Whitley CB, Belani KG, Chang PN, et al. Long-term outcome of Hurler syndrome following bone marrow transplantation. Am J Med Genet 1993; 46:209–218.
14. Peters C, Shapiro EG, Anderson J, et al. Hurler syndrome: II. Outcome of HLA-genotypically identical sibling and HLA-haploidentical related donor bone marrow transplantation in fifty-four children. The Storage Disease Collaborative Study Group. Blood 1998;91:2601–2608.
15. Souillet G, Guffon N, Maire I, et al. Outcome of 27 patients with Hurler's syndrome transplanted from either related or unrelated haematopoietic stem cell sources. Bone Marrow Transplant 2003; 31:1105–1117.
16. Rohrbach M, Clarke JT. Treatment of lysosomal storage disorders: progress with enzyme replacement therapy. Drugs 2007;67:2697–2716.
17. Munoz-Rojas MV, Vieira T, Costa R, et al. Intrathecal enzyme replacement therapy in a patient with mucopolysaccharidosis type I and symptomatic spinal cord compression. Am J Med Genet A 2008;146A:2538–2544.
18. Vera M, Le S, Kan SH, et al. Immune response to intrathecal enzyme replacement therapy in mucopolysaccharidosis I patients. Pediatr Res 2013; 74:712–720.
19. Kakkis E, McEntee M, Vogler C, et al. Intrathecal enzyme replacement therapy reduces lysosomal storage in the brain and meninges of the canine model of MPS I. Mol Genet Metab 2004;83:163–174.
20. Dickson P, McEntee M, Vogler C, et al. Intrathecal enzyme replacement therapy: successful treatment of brain disease via the cerebrospinal fluid. Mol Genet Metab 2007;91:61–68.
21. Begley DJ, Pontikis CC, Scarpa M. Lysosomal storage diseases and the blood–brain barrier. Curr Pharm Des 2008;14:1566–1580.
22. Wolf DA, Banerjee S, Hackett PB, et al. Gene therapy for neurologic manifestations of mucopolysaccharidoses. Expert Opin Drug Deliv 2015; 12:283–296.
23. Aronovich EL, Hackett PB. Lysosomal storage disease: gene therapy on both sides of the blood-brain barrier. Mol Genet Metab 2015;114:83–93.
24. Hartung SD, Frandsen JL, Pan D, et al. Correction of metabolic, craniofacial, and neurologic abnormalities in MPS I mice treated at birth with adeno-associated virus vector transducing the human alpha-L-iduronidase gene. Mol Therapy 2004;9:866–875.
25. Desmaris N, Verot L, Puech JP, et al. Prevention of neuropathology in the mouse model of Hurler syndrome. Ann Neurol 2004;56:68–76.
26. Wolf DA, Lenander AW, Nan Z, et al. Direct gene transfer to the CNS prevents emergence of neurologic disease in a murine model of mucopolysaccharidosis type I. Neurobiol Dis 2011;43: 123–133.
27. Wang D, Zhang W, Kalfa TA, et al. Reprogramming erythroid cells for lysosomal enzyme production leads to visceral and CNS cross-correction in mice with Hurler syndrome. Proc Natl Acad Sci U S A 2009;106:19958–19563.
28. Dai M, Han J, El-Amouri SS, et al. Platelets are efficient and protective depots for storage, distribution, and delivery of lysosomal enzyme in mice with Hurler syndrome. Proc Natl Acad Sci U S A 2014;111:2680–2685.
29. Ponder KP, Haskins ME. Gene therapy for mucopolysaccharidosis. Exp Op Biol Ther 2007;7:1333–1345.
30. Chung S, Ma X, Liu Y, et al. Effect of neonatal administration of a retroviral vector expressing alpha-L-iduronidase upon lysosomal storage in brain and other organs in mucopolysaccharidosis I mice. Mol Genet Metab 2007;90:181–192.
31. Traas AM, Wang P, Ma X, et al. Correction of clinical manifestations of canine mucopolysaccharidosis I with neonatal retroviral vector gene therapy. Mol Ther 2007;15:1423–1431.
32. Kobayashi H, Carbonaro D, Pepper K, et al. Neonatal gene therapy of MPS I mice by intravenous injection of a lentiviral vector. Mol Ther 2005;11:776–789.
33. Visigalli I, Delai S, Politi LS, et al. Gene therapy augments the efficacy of hematopoietic cell transplantation and fully corrects mucopolysaccharidosis type I phenotype in the mouse model. Blood 2010;116:5130–5139.
34. Janson CG, Romanova LG, Leone P, et al. Comparison of endovascular and intraventricular gene therapy with adeno-associated virus-α-L-iduronidase for Hurler disease. Neurosurgery 2014;74:99–111.
35. Hinderer C, Bell P, Gurda BL, et al. Intrathecal gene therapy corrects CNS pathology in a feline model of mucopolysaccharidosis I. Mol Ther 2014; 22:2018–2027.
36. Hinderer C, Bell P, Louboutin JP, et al. Neonatal systemic AAV induces tolerance to CNS gene therapy in MPS I dogs and nonhuman primates. Mol Ther 2015;23:1298–1307.
37. Ellinwood NM, Ausseil J, Desmaris N, et al. Safe, efficient, and reproducible gene therapy of the brain in the dog models of Sanfilippo and Hurler syndromes. Mol Ther 2011;19:251–259.
38. Wolf DA, Hanson LR, Aronovich EL, et al. Lysosomal enzyme can bypass the blood–brain barrier and reach the CNS following intranasal administration. Mol Genet Metab 2012;106:131–134.
39. Barnes CA. Memory deficits associated with senescence: a neurophysiological and behavioral study in the rat. J Comp Physiol Psychol 1979;93: 74–104.
40. Harrison FE, Hosseini AH, MacDonald MP. Endogenous anxiety and stress responses in water maze and Barnes maze spatial memory tasks. Behav Brain Res 2009;198:247–251.
41. Fratantoni JC, Hall CW, Neufeld EF. Hurler and Hunter syndromes: mutual correction of the defect in cultured fibroblasts. Science 1968;162:570–572.
42. Kornfeld S. Trafficking of lysosomal enzymes. Faseb J 1987;1:462–468.
43. Watson G, Bastacky J, Belichenko P, et al. Intrathecal administration of AAV vectors for the treatment of lysosomal storage in the brains of MPS I mice. Gene Ther 2006;13:917–925.
44. Hinderer C, Bell P, Gurda BL, et al. Liver-directed gene therapy corrects cardiovascular lesions in feline mucopolysaccharidosis type I. Proc Natl Acad Sci U S A 2014;111:14894–14899.
45. Dhuria SV, Hanson LR, Frey WH 2nd. Intranasal delivery to the central nervous system: mechanisms and experimental considerations. J Pharm Sci 2010;99:1654–1673.
46. Lochhead JJ, Thorne RG. Intranasal delivery of biologics to the central nervous system. Adv Drug Deliv Rev 2012;64:614–628.
47. Lochhead JJ, Wolak DJ, Pizzo ME, et al. Rapid transport within cerebral perivascular spaces underlies widespread tracer distribution in the brain after intranasal administration. J Cereb Blood Flow Metab 2015;35:371–381.
48. Thorne RG, Hanson LR, Ross TM, et al. Delivery of interferon-beta to the monkey nervous system following intranasal administration. Neuroscience 2008 27;152:785–797.
49. Hanson LR, Frey WH 2nd. Intranasal delivery bypasses the blood-brain barrier to target therapeutic agents to the central nervous system and treat neurodegenerative disease. BMC Neurosci 2008;9:S5.
50. Thorne RG, Pronk GJ, Padmanabhan V, et al. Delivery of insulin-like growth factor-I to the rat brain and spinal cord along olfactory and trigeminal pathways following intranasal administration. Neuroscience 2004;127:481–496.

51. Renner DB, Frey WH 2nd, Hanson LR. Intranasal delivery of siRNA to the olfactory bulbs of mice via the olfactory nerve pathway. Neurosci Lett 2012;513:193–197.

52. Harmon BT, Aly AE, Padegimas L, et al. Intranasal administration of plasmid DNA nanoparticles yields successful transfection and expression of a reporter protein in rat brain. Gene Ther 2014;21: 514–521.

53. Lemiale F, Kong WP, Akyürek LM, et al. Enhanced mucosal immunoglobulin A response of intranasal adenoviral vector human immunodeficiency virus vaccine and localization in the central nervous system. J Virol 2003;77:10078–10087.

54. Ma XC, Chu Z, Zhang XL, et al. Intranasal delivery of recombinant NT4-NAP/AAV exerts potential antidepressant effect. Neurochem Res 2016;41: 1375–1380.

55. Inagaki K, Fuess S, Storm TA, et al. Robust systemic transduction with AAV9 vectors in mice: efficient global cardiac gene transfer superior to that of AAV8. Mol Ther 2006;14:45–53.

56. Aschauer DF, Kreuz S, Rumpel S. Analysis of transduction efficiency, tropism and axonal transport of AAV serotypes 1, 2, 5, 6, 8 and 9 in the mouse brain. PLoS One 2013;8:e76310.

57. O'Keefe J, Dostrovsky J. The hippocampus as a spatial map. Preliminary evidence from unit activity in the freely-moving rat. Brain Res 1971;34:171–175.

58. O'Keefe J. Place units in the hippocampus of the freely moving rat. Exp Neurol 1976;51:78–109.

Received for publication January 1, 2017;
accepted after revision April 19, 2017.

Published online: April 20, 2017.